

INTERNATIONAL SOCIETY FOR SOIL MECHANICS AND GEOTECHNICAL ENGINEERING



This paper was downloaded from the Online Library of the International Society for Soil Mechanics and Geotechnical Engineering (ISSMGE). The library is available here:

<https://www.issmge.org/publications/online-library>

This is an open-access database that archives thousands of papers published under the Auspices of the ISSMGE and maintained by the Innovation and Development Committee of ISSMGE.

Technical Session 1c: Problematic Soils and Geosynthetic Material

Séances techniques 1c: Sols Problematique et Matériaux Geosynthetique

S. I. Kofi Ampadu,

Kwame Nkrumah University of Science and Technology, Kumasi, Ghana

1 INTRODUCTION

This session combined two themes: Problematic soils and geosynthetic materials. A total of 50 papers under 24 nationalities were submitted for this session. Of the total, 27 were on the sub-theme of problematic soils while the remaining 23 were on geosynthetic materials. Table 1-1 shows the further categorization of the papers on problematic soils. It can be seen that the papers have been grouped into 7 categories based on the soil type investigated. These groups are collapsible soils, cruseable sand, pumice and volcanic soils, residual soils, expansive soils, and peat. The last category termed “special” cover papers which do not fit any of the six categories above.

Table 1-1 Classification of Papers on Problematic Soils

Soil Category	Author	Country	Type of Investigation				
			Field	Element Test	Physical Model	Analytical	Numerical
Collapsible Soil	Meier C. Boley C. and Zou, Y.	Germany					
	Rinaldi V.A. and Capdevila J.A.	Argentina					
	Li, L., Wang S.J., Chen R., Ng C.W.W. and Li Z.	Hong Kong					
	Al-Farouk O., Al-Damijji, Al-Omari R.R., Al-Ani, M.M., Fattah M.Y.	Iraq					
	Al-Khatfaji AN, Khorshid NS, Al-Musawe MJ, Al-Obaid BM	Iraq					
	Zhakulin AS Zhakulina AA and Unabaev B.Zh	Kazakhstan					
Crusheable Sand	Hassanlourad M. Salzhzadeh H. and Shahnazari H.	Iran					
	Medeiros C. Jr, Drosenmeyer A. C.C., Muxfeldt A.S., Dutra A.B., Silveira C.A.B. and Frangov, G., Krastonov. M. and Varbanov. B.	Brazil					
		Bulgaria					
Pumice and Volcanic Soils	Badillo E.J.	Mexico					
	Kikkawa N., Pender M.J., Orense R.P. and Matsushita E.	New Zealand					
	Arthurs JM, Wilson CJN and Prebble WM, St. George, JD	New Zealand					
	Ishikawa T., Miura S. and Tokoro T.	Japan					
	Adamska K.Z. and sulewska M.J.	Poland					
Residual soils	Reiss R.M., Vilar O.M. and Azevedo R.F.	Brazil					
Expansive Soils	Omosho O.	Nigeria					
	Nowamooz h. and Masroufi F.	France					
	Farooq J. and Virk K.A.	Pakistan					
	Demeneghi A.	Mexico					
Peat	Imre, E., Moczar, B. and Farkas J.	Hungary					
	Szymanski A., Sas W. and Niesiolowska A.	Poland					
Special	Okajima K., Tanaka T., Zhusupbekov A., Baltassov T., Bazarbayev D. and Popov V.	Japan					
	Rojas J.C. and Mancuso C.	Italy					
	Talbi S., Dumont M. and Fleureau J.M.	France					
	Ajdan M., Habibagahi G. and Ghahramani A.	Iran					
	Villar L.F.S., de Campos T.M.P., Azevedo R.F., Zornberg J.G.	Brazil					
	Bicalho K.V., Marinho F.A.M., Fleureau J.M., Correia A.G. and Ferreira S.	Brazil					

This included 5 papers on unsaturated soil mechanics and one paper on deformation of sheet pile.

The 23 papers on geosynthetic materials have been subdivided according to area of engineering application as shown in Table 1-2. The tools used for the investigation have also been indicated. The categories are landfill systems, pavements, dams, embankments on soft ground, bearing capacity of shallow foundations, reinforced walls and “special” which consist of papers with general application.

Table 1-2 Classification of Papers on Geosynthetics

Application	Author	Country	Type of Investigation				
			Field	Element Test	Physical Model	Analytical	Numerical
Landfill Systems	Pitanga, H.N., Vilar O.M. and Goure J.P.	Brazil					
	Mazzieri F., Pasqualini E., DiEmidio G., Van Impe W.F.	Belgium					
	Du, Y.J., Liu, S.Y. and Shen S.L.	China					
Pavements	Han, J., Bhandari and Parsons R.L.	USA					
	Zornberg J.G. & Gupta R.	USA					
Dams	Pimentel V.E., Benjamin C.V.S., Franco D. and Franca P.	Brazil					
	Beirigo E.A., Gardoni M. G. and Palmeira E.M.	Brazil					
Embankments on soft ground	Ye Y.S., Cai D.G., Zhang Q.L. and Yan H.Y.	China					
	Araujo G.L.S., Palmeira E.M., Cunha R.P.	Brazil					
	Al-Adili A., Chandra S., Sivakugan N.	Iraq					
Bearing Capacity of Shallow Foundations	Casagrande M. D.T., Consoli N.C. and Thome A.	Brazil					
	Zhusupbekov A., Lukpanov R., Muzdybaeva T., Das B.M., Patra C.R., Shin E.C.	Kazakhstan					
	Nakai T., shahin H.M., Watanabe A. and Yonaha S.	Japan					
	Puri V.K., Kumar S., Das B.M., Prakash S. and Yeo B.	USA					
	Sayao ASFJ, Nunes ALLS, Becker LDB and Siera ACCF	Brazil					
Reinforced Walls	Luking J. and Kempfert H.G.	Germany					
	Hafz N. and Sadr A.	Iran					
Special	Khan A.J., Siddiquee MSA, Noor MA, Mahaseth B.	Bangladesh					
	Atmztzidis D.K., Chryssikos DA and Papaelstathion I.M.	Greece					
	Carneiro J.R., Almeida, P.J. and Lopes M.L.	Portugal					
	El-Sherbiny R. and Gross B.	USA					
	Mendez B., Botero E. and Romo M.P.	Mexico					
Kavazanjian E., Jr, Iglesias E. and Karatas I.	USA						

The next session covers a review of the individual papers under problematic soils while section 3 covers those on geosynthetic materials. For each section, a brief overview of each paper is included summarizing some of the key issues and conclusions.

2 PROBLEMATIC SOILS

2.1 Collapsible Soils (Salt bearing Soils)

Under the general theme of collapsible soils, 6 papers were presented. 3 papers were on the material referred to as loess while 3 papers were on gypseous soils. Loess has a weak cementation given by the presence of soluble salts, silica amorphous, calcium carbonate, gypsum and iron oxide distributed at particle contacts and also concentrated as nodules. Pore fluid has significant effect on loess stability. Highly acidic leachate dissolves carbonates while alkaline water promote development of silica bonding in presence of hydroxides (Rinaldi and Capdevila, 2009).

Gypseous soils have high concentration of calcium sulphate. When dry the gypsum fills all the pore spaces and thus provide connection making it stiff. When they come into contact with water, however, they undergo loss of strength and increase in compressibility due to the water washing out the soluble sulphate leading to progressive collapse of structure. The dissolution of calcium sulphate leads to karst hazards

2.1.1 Loess

Meier C. Boley C. and Zou, Y., investigated the collapse behaviour and microstructure of loess soils in Afghanistan. Their study sought to investigate the collapse behaviour of loess under static loading and to provide a chemical basis for understanding the collapse. They performed the collapse test in the oedometer test apparatus. They analysed the mineralogical composition using the X-ray diffraction test and the microstructure using the electron Microscope. They also used chemical test to determine the lime content and used ion exclusion analysis to confirm the presence of CaCO₃. The results of X-ray diffraction showed that carbonate (calcite and dolomite) constituted about 37% while quartz crystals constituted 16%. The microscope visual images confirmed the collapse of microstructure and the chemical analysis confirmed that part of collapse was due to solution of lime and salt.

Rinaldi V.A. and Capdevila J.A. from Argentina investigated the effect of sampling disturbance on the stress strain behaviour of a saturated loess from Argentina. They performed both plate loading test (PLT) and insitu shear wave velocity test using the cross hole method in the field. In the laboratory they used block samples and performed the oedometer test modified to include bender elements for shear wave velocity measurement. They also performed triaxial tests (TX) measuring displacements with LDT and measured suction using water tensiometer imbedded in the block sample. They concluded that when measured at the same strain, the secant modulus E_{sec} values from PLT and TX agree. That block sampling gives fair representation of loess properties. They however warned that the presence of cemented aggregates may increase shear wave velocity in thin samples, hence shear wave velocity in field and laboratory may be different (scale effect). Consequently, the size of samples used for laboratory testing should be large compared with sized of nodules distributed in loess.

Li, L. Wang S.J. Chen R., Ng C.W.W. and Li Z., report from Hong Kong that potassium silicate can be used to reinforce loess soils and proceed to investigate the reinforcement mechanism and effect of potassium silicate (PS) solutions in improving the characteristics of loess. In their study they investigated 3% and 7% potassium silicate stabilized and non-stabilized compacted loess soils under both saturated and unsaturated conditions. The unsaturated condition was created in the samples by subjecting prepared samples to drying in ambient condition while the saturation to simulate effect of rainfall was done in a triaxial cell. The strength was determined under the unconsolidated Undrained TX compression. They

used Scanning electron microscopy (SEM) and Transmission Electron Microscopy (TEM) for microscopic characteristics of the reinforced material. They concluded that PS reinforces loess soils and that PS reinforcement does not affect permeability. They showed that PS reinforcement increases both peak and residual strength. They also concluded from the SEM and TEM results that PS reinforcement gives loess a reticular and dense structure resulting from PS reaction with clay minerals to produce crystalline and non-crystalline structures, which is resistant to (water) rainfall.

2.1.2 Gypseous Soils

Al-Farouk O. Al-Damijji, Al-Omari R.R. Al-Ani, M.M. Fattah M.Y., conducted Experimental and numerical investigation into the dissolution of gypsum (Calcium Sulphate CaSO₄) in gypiferous soils of Iraq which occurred as sandy soil with gypsum content more than 60%. In the experimental study they conducted the leaching and consolidation test in the Oedometer apparatus modified for permeability measurement and varied the gypsum content of the flowing water from 0.25 to 1.0g/l. They observed that leaching strain variation with time reduced significantly with increasing gypsum content and that the void ratio is independent of the leaching process but that the porosity varied during the leaching. They then conducted Coupled FEM analysis and concluded that large displacement occurred near the surface and that the dissolution of gypsum decreases with depth.

Al-Khafaji AN, Khorshid NS, Al-Musawe MJ, Al-Obaid BM performed plate loading tests on two types of gypseous soils of different physical properties from Iraq. The material investigated were Silty to sandy gravel (GM) and Cemented silty sand (SM). The Field Plate Loading Test was conducted under soaked and unsoaked conditions using an 80cm test plate and a 50 ton hydraulic jack and soaking under 30cm deep of water for 7-11 days. They evaluated various moduli from the load-settlement curves. They based their analysis on the elastic equation

$$E = \frac{\pi D q}{4 \rho} (1 - v^2) \quad \text{Equation 2-1}$$

The initial tangent moduli E_i ($q=0$ and $\rho=0$) and assuming $v=0$ was evaluated using a hyperbolic curve fitting, for which a is the y-intercept of the ρ/q vrs ρ plot.

$$E_i = \frac{\pi D}{4} \frac{dq}{d\rho} \quad \text{Equation 2-2}$$

$$E_i = \frac{\pi D}{4} \frac{1}{a} \quad \text{Equation 2-3}$$

Using the above method, they evaluated the average E_i and concluded that Silty gravel had higher E values than silty sand for both natural and soaked values and that soaking decreases stiffness moduli of gypsiferous soils and increases settlement 2-3.5 times for SM and 2-5 times for GP-GM soils

Zhakulin AS Zhakulina AA and Unaibaev B.Zh from Kazakhstan conducted analysis of the relationship between the settlement and the volume of water-soluble salts leached out in a multilayer salt-bearing soil. In order to define the connection between the volume of salts washed out by filtration flow and suffusion setting at any stage of soil leaching, they introduced a new dimensionless parameter – coefficient of replacement k_{zi} ,

which showed which part of the volume change is replaced by non-soluble particles of soil, (Verigin, 1979):

$$k_{zi} = \frac{\delta \cdot \varepsilon_{s.f.i.}}{\beta_i \cdot D_0 \cdot \gamma_{dc}} \quad \text{Equation 2-4}$$

where $\varepsilon_{s.f.i.}$ - relative suffusion soil compressibility under given pressure P_i ; β_i - degree of soil leaching being equal to ratio of leached from soil salts weight to their initial weight, unit fractions; D_0 - initial weight degree of soil salinity, unit fractions.; δ - salts density, g/cm^3 .

Defining ξ_0 - initial specific volume of salts in soil; $\xi(t)$ - specific volume of rest salts in soil per time t , they established the following dependence between relative suffusion deformation and volume of washed out salts.

$$\varepsilon_s(t) = k_z [\xi_0 - \xi(t)]$$

They integrated this between the thickness of the salt-bearing layer. When within a layer k_z varied significantly, the layer was divided into sublayers and the ε_s values obtained by summation. They developed a computer programme for the computation and applied it to a layered soil consisting of a plastered clay sand and light loam .

2.2 Crusheable Sand

The crusheable sands category consists of calcerous sand of biological origin. They are naturally cemented to varying degrees and the sand particles crush under load. Thus piles driven in calcareous sand may have relatively very low friction values compared to noncalcerous sand such as siliceous sand.

Hassanlourad M. Salchzadeh H. and Shahnazari H., from Iran investigated the strength of chemically grouted micro pile model in calcareous sand. The calcerous sand had about 95% $CaCO_3$ content and was grouted with Sodium Silicate. The used a physical Model micropile loading test and laboratory unconfined Compressive strength test. The optimum water: silicate (W/S) ratio to give max q_u and stiffness $(E_{tan})_{initial}$ was found to be 0.5. Increasing initial Dr of grouted sand increases q_u and $(E_{tan})_{initial}$. The conclusion was that chemical grouting can compensate for effect of crushing in calcerous sand and that grouting increases bearing capacity of calcerous sand by between 5.4 for $Dr=0.8$ to 35 times for $Dr=0.2$

Medeiros C. Jr, Drose Meyer A. C.C. Muxfeldt A.S., Dutra A.B. Silveira C.A.B. and Sants R.M. performed a geotechnical characterization of calcerous soils for pile foundation design of offshore production platforms off the coast of Brazil. They conducted offshore sampling from boreholes in 100m of water advanced by rotary drilling and sampling by wireline percussion. Within the boreholes they conducted Piezocone test. Samples retrieved were subjected to routine laboratory tests as well as chemical test to determine the $CaCO_3$ content. Direct shear tests to determine steel/soil friction as well as isotropic compressibility tests in triaxial apparatus were performed.

Their results showed that Brazilian calcerous sand has $CaCO_3$ content of about 27% which is much lower than those forming the basis of current Brazilian design standard. They observed that Current practice for dimensioning and installation of piles in calcerous soils in Brazil based on recommendations from international literature overestimate pile lengths and proceeded to propose the use of the coefficient of compressibility for determination of the limiting shaft friction for design.

Frangov, G., Krastonov. M. and Varbanov. B. reported on the Complex engineering geological conditions for civil

construction in the Rhodope Mountain of Bulgaria. The location was a carbonate terrain . They conducted engineering geological mapping, borehole drilling, continuous electrical profiling (electromyography) and routine laboratory tests as part of a subsurface geotechnical investigation for a resort project. The specific types of strength tests were not mentioned. The paper described the geological-tectonic structure as well as the hydrogeological conditions at the site. The lessons from subsurface investigation was that there is large variation in rock and soil properties within short distances and that special attention needs to be paid to investigation in carbonate terrains due to probable existence of karst formed in different sizes and spatial distributions. In addition, water in the karst had a slight carbonic acid aggressiveness towards concrete.

Badillo E.J. from Mexico presented a mathematical characterization of pumice and quartz sands. His presentation was in response to attempting to bridge the gap between academic and practice as discussed in the 16th ICSMGE. His paper was an analytical approach applying the Principle of Natural Proportionality to explain (model) the different behavior observed between quartz sand and pumice subjected to controlled CPT test in laboratory. He determined the coefficients of the equations derived from test data He concluded that sands subjected to drained TX behave like clays with particle interlocking representing over consolidation effect.

2.3 Pumice and Volcanic soils

Pumice and volcanic material are initially distributed by volcanic eruption and transported by air followed by erosion and river transport. It has both internal and external voids and can easily be crushed. Crushing of particles lead to increase in voids. They have low natural densities. Pumice sand is characterized by soft vesicular grains of low crushing strength giving the material high void ratios and high compressibility. Conventional relationship between the CPT q_c relative density and confining stress are not valid for pumice soils

Kikkawa N. Pender M.J., Orense R.P. and Matsushita E. investigated the behaviour of pumice sand from New Zealand during hydrostatic and K_0 compression. They used X-ray CT scan, grading Analysis as well as Hydrostatic and K_0 compression test in Triaxial Apparatus for their investigation. Typical pumice particle is shown in Fig 2-1

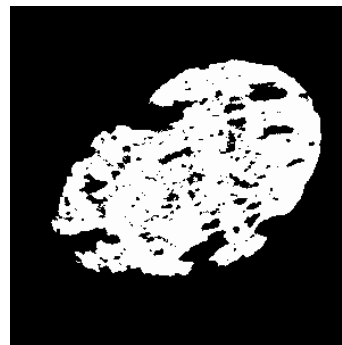


Fig. 2-1 Cross sectional binary image of pumice particle (Kikkawa et al 2009)

The densities obtained ranged from 552 to 704 kg/m^3 . For the stress relaxation test, they applied a cell pressure of 50kPa and compressed the sample at rates ranging between 0.5mm/min-25mm/sec until axial deformation of 50mm. The axial deformation of 50mm was held constant and the axial stress and confining pressure were monitored with time. They computed particle breakage using the definition of total particle breakage proposed by Hardin (1985) which uses the area under the particle size distribution curve between defined boundaries.

Their defined boundary was 0.063mm. Using this they concluded that substantial particle crushing occurred under shear stresses (from K_0 testing) but insignificant crushing occurred under volumetric compression. They postulated based on their results of the effect of density and displacement rate that it will be possible to evaluate the density of pumice sand through the magnitude of stress relaxation during CPT test.

Arthur JM, Wilson CJN and Prebble WM, St. George, JD reported on a study of the Sensitivity in volcanoclastic silts in North Island of New Zealand. The material was clayey silt with very fine sand sized pumice fragments. Such soils are known to pose slope Stability problems. Their investigation was a laboratory investigation. The tests they performed included physical property tests, the drained and Undrained Triaxial Shear as well as the Ring Shear Test. In addition, they performed the X-ray Diffraction test for clay mineralogy and Scanning Electron Microscope for microstructure. Their results showed that the predominant group of minerals is kaolin group minerals (halloysite and kaolinite) and the microstructure was similar to matrix microstructure clay.

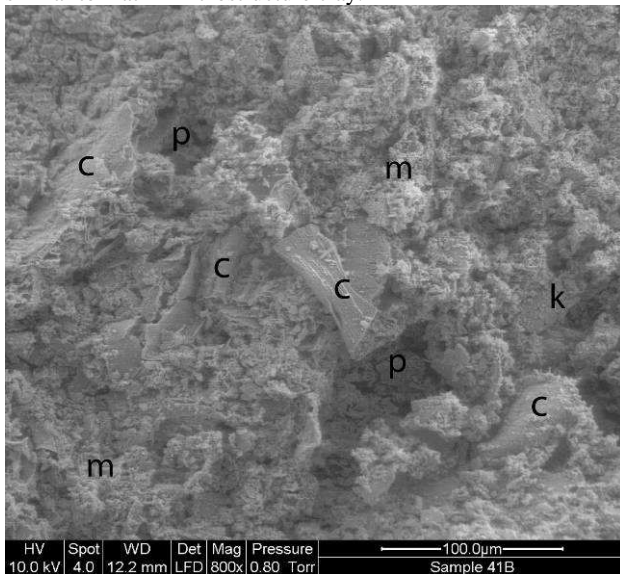


Figure 8 - SEM photomicrograph of sample 41 from Pahoia. c - crystal grain, m - clay matrix, p - pore, k - kaolin microaggregate. (Arthur et al 2009)

The sensitivity was shown in a Peak Angle of 30° with a residual angle of 15° . They noted that the Shear vane is not suitable for measuring actual shear strength of the volcanoclastic silts. They noted that New Zealand sensitive soils originate from volcanic silts dominated by glass and crystals and consequently behave like silts where the original glass has been weathered to form clay minerals. In contrast the Canadian and Norwegian sensitive soils are glacial derived sediments deposited in estuarine environments which had undergone little weathering. They behave like clays. However both are young and normally consolidated

Ishikawa T., Miura S. and Tokoro T. reported on developing testing methodology for evaluating the effect of freeze-thaw action on hydromechanical behaviour of unsaturated granular materials. The focus of their study was on two newly developed apparatus: the freeze-thawing triaxial test apparatus and the freeze-thawing permeability test apparatus. Previous equipment used by the first author could not measure the frost heave characteristics. One feature of the triaxial system is that it has a cooling system to control the temperature in the cap and pedestal independently. Secondly, one dimensional frost heave can be simulated in the apparatus in addition to monotonic

triaxial compression test and water retention test. It is capable of independent control of pore air pressure (u_a) and pore water pressure (u_w). They used crushable volcanic coarse-grained material of insitu density $0.53-0.55 \text{ g/cm}^3$. Their results showed that one cycle of freeze-thaw give higher suction and lower coefficient of permeability than non freeze-thaw ones for the same degree of saturation. The conclusion is that freeze-thaw action has strong influence on hydromechanical behaviour of crushable volcanic coarse-grained soil.

Adamska K.Z and sulewska M.J. from Poland performed Artificial Neural modeling of CBR values for compacted fly ash. Using fly ash (sandy silt) from hard coal burning in Thermal-Electric Power Plant they performed Laboratory CBR Test on Standard Proctor and Modified Proctor compacted unsaturated and 4-days saturated samples. They had previously established that statistically the correlation between the set of parameters derived from the particle size distribution, the compaction method, the state of saturation and the compactibility on the one hand and CBR on the other was low. Therefore they applied the Artificial Neural Network with Multi-Layer Perception (MPL) incorporating one hidden layer. The Neural network had an 8-5-1 architecture (8 input, 5 neurons in hidden layer and 1 output). The STATISTICA Neural Networks software was used. The data set was made up of a Learning subset ($L=70$), Validating subset ($V=35$) and Testing subset ($T=35$). They confirmed that the CBR is a function of the water content and that unsaturated samples attained maximum CBR for $w=w_{opt}-5\%$ while saturated samples had maximum CBR at $w < w_{opt}$. For the dry density their results showed that the CBR is a function of ρ/ρ_{dmax} and also $\rho-\rho_{dmax}$. They concluded that the variables ρ_d and w/w_{opt} were significant parameters.

2.4 Residual Soils

Reiss R.M., Vilar O.M. and Azevedo R.F. from Brazil discussed the Stress-strain behaviour of a residual soil profile from gneiss. They investigated and compared the behaviour of two types of soils both derived from gneiss rock: a "young" and a "mature" residual soil according to the nomenclature by Vergas (1953) or a "saprolite" from horizon 1C and soil from horizon 1A and 1B according to Deere & Patton (1971). They conducted conventional, drained, stress path controlled and isotropic compression triaxial tests as well as triaxial tests with matric suction control loading the samples vertical, parallel and perpendicular to the shistosity as shown in Fig.2-2.

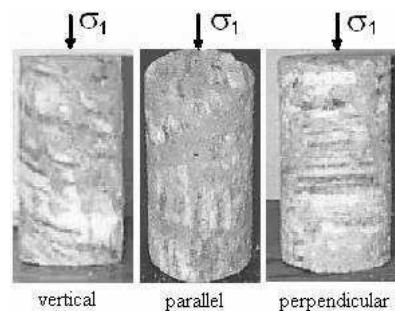


Fig. 2-2 Directions of loading of young residual soil (Reiss et al 2009)

The young (saprolite) residual soil despite visible shistosity showed isotropic behaviour with respect to deformability and strength while the mature soil which does not present any visible characteristic inherited from parent rock and visually seems to be more homogeneous had anisotropic behaviour. They showed that for the two soils, ϕ' was independent of matric suction, ψ , and did not vary with the loading direction. On the other hand the cohesion varied slightly with loading

direction and the $c-\psi$ relationship was hyperbolic as suggested by Rohm & Vilar (1995)

$$c(\psi) = c' + \frac{\psi}{a + b\psi} \quad \text{Equation 2-5}$$

2.5 Expansive Soils

Expansive soils undergo volumetric increase when they come into contact with water and volumetric decrease when they undergo drying. This means that structures founded on expansive soils undergo stress reversals with wetting and drying cycles. The cause of expansive behaviour is believed to be the presence of the montmorillonite clay mineral. The mechanism for the volumetric changes is explained as when a molecule of water is introduced into two platelets of a soil particle, its electric charges are pulled apart, becoming more dipolar and attracting other water molecules, additionally, the electric charges on the surface of the platelets also concentrate, pushing away other platelets and increasing the number of molecules between them, resulting in the increase of the volume of the particles (Alonso 2008). When suction decreases, the double layer of the particles increases. Thus soil undergoes volumetric changes from variation in suction.

Omotosho O. reported on the response of expansive deltaic soils of the Niger Delta to stabilization with CaCl_2 and Lime and the effect of cement on CaCl_2 stabilized soil. He performed 24-hr free swell test. Standard Proctor Compaction and soaked CBR test on 27 samples retrieved from 18 sites scattered in the fresh water zone of the Niger delta. The PI of the samples ranged between 7.1% and 46.2 while the clay content varied between 18.6% and 31.5%. He tested various criteria for identification of expansive soils on the soils and observed that the PI-based criteria (Skempton 1953, O’Neil & Poormoayed, 1980) are not suitable for identifying active deltaic soils. He concluded that CaCl_2 is more effective than Lime in limiting free swell at small stabilizer content (Fig 2-3). However at higher stabilizer contents (equal to and probably greater than 12%), it appears that the effect of both stabilizers on the free swell of all soil samples tend to converge. He presented a method for selecting stabilizer content to achieve 2.5% free swell. He explained that the stabilizers – through ion-exchange reaction – attracted and absorbed the water molecules at the crystal/plate boundary and precipitate relevant chemical compounds to seal off the interface from further water ingress and thus reduced the swell.

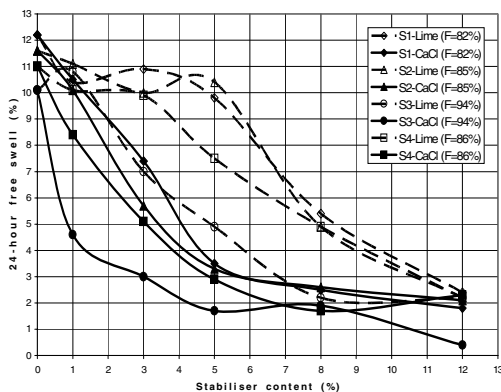


Fig. 2-3 Free swell and stabilizer content (after Omotosho & Ogboin, 2009)

Farooq J and Virk K.A., investigated the improvement in engineering characteristics of an expansive clay from Daska in Sialkot district of Pakistan by mixing with sand. The clay had

a sand content of 27% and a silt and clay content of 73% as well as a liquid limit of 38 and a plasticity index of 20. They mixed samples of expansive clay with various percentages of river sand ranging from 0-35%. They evaluated the mechanical properties using the modified AASHTO compaction, the CBR Test and the One-Dimensional Consolidation Test. In the one-dimensional consolidation test they flooded the sample against a seating pressure of 7kPa and allowed the sample to swell measuring deformation with time until no further deformation occurs. They then computed the Percent Swell as increase in vertical height expressed as % original height. They then loaded the swelled specimen in increments until swelling is reduced to zero and obtained the Swell Pressure as the load required. Finally they loaded the sample in increments to maximum of 3435kPa and measured the consolidation characteristics.

Their results showed that the stabilization with sand improves MDD and that the CBR increases linearly with sand content from 4% to 8% at a sand content of 35%. The Swell potential reduces from 3.5% to 0.5% and Swell Pressure reduces from 90kPa to 10 kPa at 35% sand content. Both the LL and PI reduced with increasing sand content.

Demeneghi A., from Mexico presented an analytical method for estimating the deformations in expansive clays. In his approach he derived constitutive equations based on the assumption that the deformation of expansive soils is the algebraic sum of compression caused by external load increments and deformation produced by suction changes in the soil. He derived equation for the computation of compression, δ_z , caused by external load increments for loading either along recompression line (Equation 2-6) or normally consolidation line (Equation 2-7) for strains ϵ_{va} , due to adsorption of water molecules in soil particles (Equation 2-8)

$$\delta_z = \left[1 - \left(\frac{p_{beo} + c\sigma_z}{p_{beo}} \right)^{-f/cAs} \right] (\Delta\epsilon_o) \quad \text{Equation 2-6}$$

$$\delta_z = \left[1 - \left(\frac{p_{beo} + c\sigma_z}{p_{beo}} \right)^{-f/cAvr} \right] (\Delta\epsilon_o) \quad \text{Equation 2-7}$$

$$\epsilon_{va} = 1 - \left(\frac{p_c + b_4 p_{sf}}{p_c + b_4 p_{so}} \right)^{-1/B_a} \quad \text{Equation 2-8}$$

Where p_{beo} is the initial confinement pressure for a cemented soil subjected to soil suction p_s . He outlined methods for the determining the various parameters in the equations and presented an example for the determination of the soil parameters from the oedometer test results. Finally he applied the analytical procedure to the evaluation of the settlement of a structure founded on an expansive clay layer underlying a 0.6m thick layer of sand.

Nowamooz h. and Masrouri F. from France presented a study titled “Hydromechanical behaviour of expansive soils during eh wetting and drying cycles. The article presents an experimental study performed on compacted loose and natural dense expansive soils using osmotic oedometers. Several successive cycles were applied under three different low constant vertical net stresses. The loose soil shows a significant shrinkage accumulation while the dense one produces the swelling accumulation during the suction cycles. The suction cycles induced an equilibrium stage which indicates an elastic behaviour of the samples. At the end of suction cycles, a loading/unloading test was performed at three constant suctions

for both materials. The mechanical parameters, i.e. the virgin compression index $\lambda(s)$, the apparent preconsolidation stress $p_0(s)$ and the elastic compression index values κ are completely dependent on the stress paths that was used. The whole experimental results made it possible to define the yielding surfaces: loading collapse (LC) and saturation curve (SCS). The yielding surface representing this pressure as a function of suction is called the saturation curve (SCS). Generally we can state that the suction cycles unified the LC and SCS surfaces.

2.6 Peat

Peat is derived from organic soils. They show high organic matter content, high natural water content and high void ratios. Consequently they are highly compressible.

Imre, E. Moczar, B and Farkas J. from Hungary investigated the response of peat to laboratory creep and relaxation after partial unloading. They conducted Multi-Stage oedometer Compression test, undrained Triaxial Creep Test on peat samples. The samples were highly compressible with organic content of 60-90%, high water content 300-600% and high void ratios 3.9-7.0. They observed that creep stops after partial unloading then continues after a pause. Then assuming that after a rebound displacement Δv (or void ratio increase of Δe) the pause time is equal to the time necessary for the development of the same sized creep settlement as shown in Fig. 2-4, they developed Equation 2-9 from which the pause time t_{pause} can be evaluated.

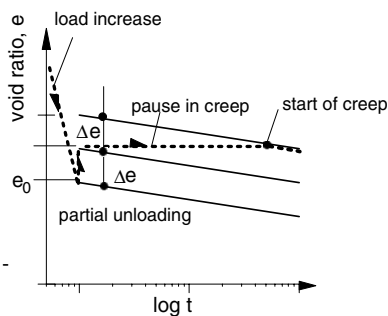


Fig. 2-4 Model for the computation of pause time (Imre et al 2009)

$$\Delta v - C'_\alpha \log \frac{t_{pause} + t_0}{t_0} = 0 \quad (2-9)$$

where C'_α is the slope of the creep settlement-log time plot.

Szymanski A., Sas W. and Niesiolowska A. from Poland conducted embankment settlement analysis on a soft organic soil using both a field and laboratory methods. The subsoil profile at the study site consisted of an amorphous peat with organic content of 80% ($w_n=310-380\%$, $LL=315-340$, $PL 140-190$, $\rho_{dry}=0.26-0.28$) on top of a Calcerous sand of organic content of 27% to 35% ($w_n=110-115\%$, $LL=110-120$, $PL 50-55$, $\rho_{dry}=0.67-0.68$).

For the field investigation they built two 4m high well instrumented embankments. They measured the vertical settlement by several settlement gauges located at various points in the embankment, the pore pressure by piezometers and horizontal displacements by inclinometers.

They took undisturbed samples of peat and calcerous sand by Shelby tube and subjected these samples to undrained and drained triaxial compression tests under different confining pressures as well as creep test under deviatoric stress of 40-70kPa. From their results they computed the coefficients of the undrained and drained Young Moduli given in Equation 2-10

$$E_u = \beta_0 q^{\beta_1} \sigma_c^{\beta_2} \quad E = \alpha_0 \sigma_1^{\alpha_1} \sigma_3^{\alpha_2} \quad \text{Equation 2-10}$$

Their results showed that E and E_u are functions of both stress range and stress history and that there is significant creep component in the measured vertical and horizontal strains. They observed large and non-linear deformations and concluded that organic subsoil performance prediction using Consolidation theory should take into account varying soil parameters (which are functions of effective stress and pre-consolidation) and large strain analysis.

2.7 Special

This category of papers did not directly address problematic soils. It consisted of 5 papers on unsaturated soil mechanics and 1 paper on deformation of sheet pile coffer dam.

Okajima K. Tanaka T Zhusupbekov A, Baitassov T. Bazarbayev D. and Popov V., presented the results of an elasto-plastic FEM modeling of the deformation of a sheet pile cofferdam used for the construction of a theatre in St. Petersburg city. The coffer dam consisted of 22.5m deep sheet pile with struts at 1.5m, 3m and 6m. The investigation was conducted with an excavation 13m wide and 12m deep. For this excavation they monitored the deformation of the sheet pile. Then they modeled the excavation using FEM analysis based on elastoplastic total stress. For the modeling they used the subsurface profile from field boring which indicated soils of varying characteristics with SPT N value ranging from 2 to 30 and assumed the subsurface soil to be cohesive. The excavation was simulated by deleting one layer at a time and computing the deformation of the sheet pile. The FEM computed displacement followed the general trend of measured displacement but the magnitude was lower

Rojas J.C. and Mancuso C., investigated the effect of loading rate on the behaviour of unsaturated soils. For their study they used reconstituted non-plastic silty sand and tested it in their custom developed unsaturated Stress Path triaxial apparatus (USPv2) capable of suction controlled tests. They performed tests under isotropic compression and shearing under suction ranging from 0 to 300kPa. For the isotropic compression test a loading rate ranging between 8 and 128 kPa/hr was used. For the tests that were sheared, a constant loading rate of 32kPa/hr was used for the isotropic compression stage while the shearing was done at a strain rate of 0.25%/hr and 2.5%/hr. Their results showed that loading rates have insignificant effect on specific volume variations at low suction of 15 to 45 kPa but becomes significant for suction of 300kPa. They also observed that the higher loading rate gave lower compressibility.

Ajdari M. Habibagahi G. and Ghahramani A., from Iran reported on their study to predict the effective stress parameter χ of unsaturated soils in plane strain condition using neural networks. The application of Bishop's effective stress for unsaturated soils depend critically on evaluating the value of the effective stress parameter χ .

$$\sigma' = (\sigma - u_a) + \chi(u_a - u_w) \quad \text{Equation 2-11}$$

The authors used a neural network with a 6-6-1 architecture and trained the ANN using 58 Consolidated Drained (CD) direct shear test results, and tested using another subset of 12 CD direct shear test results. A feed forward back propagation algorithm was used to investigate the ability of artificial neural network method for determination of χ . The 6 input neurons consisted of the saturated volumetric water content, θ_s , bubbling pressure, $(u_a - u_w)_b$, and residual water content, θ_r , the fitting parameter λ , net vertical stress and suction. Most of the parameters were obtained from soil-water characteristic curve

They concluded that the ANN model gives a good prediction of the value of χ . However the parameter is strongly dependent on the net mean stress. They noted that their study is applicable for bubbling pressure not exceeding 250kpa and to drained tests only.

Villar LFS, de Campos TMP, Azevedo R.F. Zornberg J.G. from Brazil investigated Tensile strength changes under drying and its correlations with total and matric suctions. They used a silty clay soil sample normally consolidated using two saturation fluids; a pH13 neutralized soil and pH8 non-neutralized soil to generate high osmotic suction so as to give distinct values of matric suction and total suction. They prepared cylindrical samples, initially saturated with the saturation fluids and then air dried to different water contents. They then measured the vertical loads and displacement in diametric compression test (Brazilian Test) and indirect tensile test. The results (Fig 2-5) showed among other things that there exist a linear relationship between the normalized tensile strength and both matric and total suction up to a degree of saturation of circa to 86% which corresponded to the point on the soil moisture retention curve where the curve of total suction presents its maximum curvature. This change in behavior occurred where the total suction also changed, suggesting that total suction rather than matric suction governs the response of the soil in relation to the tensile strength.

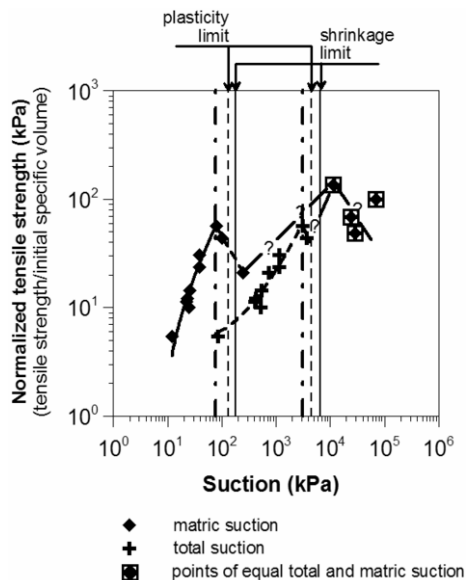


Fig. 2-5 Normalized tensile strength and suction of the neutralized soil (Villar et al 2009)

Bicalho K.V. Marinho FAM Fleureau J.M. Correia A.G. and Ferreira S. from Brazil conducted an investigation titled "Evaluation of filter paper calibrations for indirect determination of soil suctions of an unsaturated compacted silty sand". The soil used was a residual silty sand: LL=32.6, PL=25, clay=2.5%, $G_s=2.66$, OMC=17.6%, $\gamma_{dry}=18.6\text{kN/m}^3$ sieved through 0.425mm. They measured the matric suction using samples compacted at OMC and Watman 42 filter paper and computed the matric suction values using the correlation by Chandler et al 1992, ASTM D5298, and Fleureau et al 2002. Fig 2-5 shows part of their results showing the relationship between the matric suction as computed by different methods and the degree of saturation. They observed that the FPM offers a simple method of determination of soil suction but the matric suction inferred depends on the calibration curve

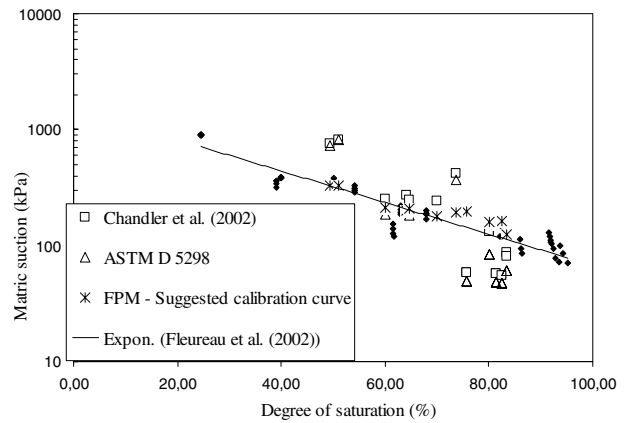


Fig. 2-6 Effect of the filter paper (FPM) calibrations on the derived soil suctions for compacted Perafita sand specimens.(Bicalho et al 2009)

Taibi S., Dumont M. and Fleureau J.M. from France reported on their investigation titled "Effective stress extended to unsaturated soils-effect of the interfaces parameters". They noted that the concept of "effective stress extended to unsaturated soils" is used in the formulation of the constitutive laws of elastic as well as elastoplastic solid phases, and controls the stress-strain relations, the volume changes and the strength of the solid skeleton, independently of the amplitude of the pore water pressure. Several researchers have shown that the extended effective stress concept remains an effective tool to describe qualitatively and quantitatively the unified mechanical behavior of the soils, assuring continuity between saturated and unsaturated domains. The paper presents the effect of the air-water surface tension and wettability of the solid particles by the liquid in the formulation of the capillary force between the particles; this force, integrated in a representative elementary volume (REV), makes it possible to define a "capillary" stress $\sigma_{cap}(p_c)$, function of the capillary pressure p_c . Taking into account the surface tension in the formulation of the capillary stress σ_{cap} is far from being negligible. Whereas this effect is negligible when the water content tends towards 0, it quickly becomes very important when the water content reaches a few percents. Validations were carried out on drying-wetting and triaxial paths on clayey sand, a kaolinite and a porous rock composed of cemented "grains"

3 GEOSYNTHETIC MATERIALS

3.1 Landfill Systems

Pitanga, H.N. Vilar O.M. and Goure J.P., from Brazil reported on "Compacted soil shear strength characterization on inclined plane test". They investigated compacted soil-geosynthetic interface and compared it with compacted soil-soil interfaces for different compaction conditions under low normal stress conditions. Their study finds application in landfill cover systems where steep slopes and low normal stresses are common. They used the Inclined Plane Test (IPT). Fig 3-1. since the direct shear test which is normally used to measure interface shear resistance does not easily accommodate the very low normal stress levels required. They investigated two geosynthetic; an HDPE Geomembrane 1.5mm thick and a nonwoven needlepunched geotextile 1mm thick and the soil is a silty sand. The prepared sample imposed a normal stress σ_v of between 2.8 kPa, and 10.4 kPa.

They observed that the failure surface can occur within the soil if the cover soil is poorly compacted. They concluded that appropriate compaction can increase the angle of resistance and hence the stability of cover system

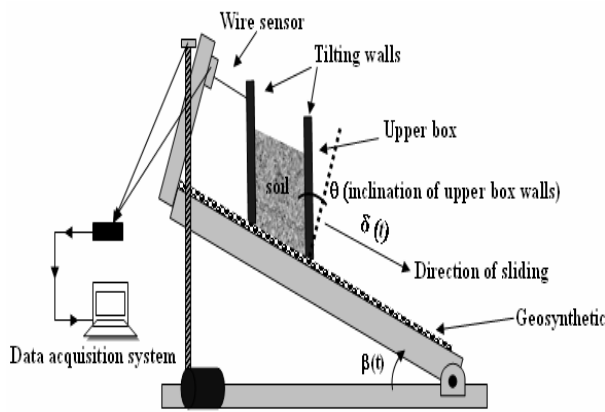


Fig. 3-1 IPT for tests on soil-geosynthetic (Pitanga et al. 2009)

Mazzieri F., Pasqualini E. DiEmidio G., Van Impe W.F. in Belgium conducted hydraulic conductivity studies on a dense prehydrated Geosynthetic Clay Liners (GCL) subjected to partial desiccation. The authors observed that the hydraulic performances of GCLs that consist of a thin layer of bentonite sandwiched between two geotextiles depend on the low hydraulic conductivity of sodium bentonite. However it is known that under field conditions, calcium can replace sodium and if this is combined with desiccation and cracking of the bentonite, the hydraulic conductivity of GCLs can increase drastically. To overcome this problem Dense Prehydrated (DPH) GCL have been recently proposed as an alternative. The study therefore sought to obtain information on the occurrence of exchange of sodium for calcium and to examine the behaviour of the DPH GCL subjected to increasingly severe drying states. To achieve this the researchers conducted long term hydraulic conductivity tests on samples of Dense PreHydrated Geosynthetic Clay Liner (DPH GCL) in a Flexible wall permeameter under a 12.5mM CaCl_2 solution and an effective stress of 15kPa. The samples were then dehydrated in thermostatic chamber at 35°C and Relative Humidity 20-40% to different water contents ranging from 35% to 85% under a vertical pressure 12.5kPa. The sample was then transferred to permeameter and rehydrated. The results showed that there was release of sodium during permeation and this was ascribed to cation exchange with calcium. The Hydraulic conductivity of DPH GCL remained low less than 2×10^{-9} cm/s for dehydration water contents exceeding the manufacturing water content of 45%. However, for water content less than 45% hydraulic conductivity increased irreversibly due to the development of unhealed cracks

Du, Y.J., Liu, S.Y. and Shen S.L. from China evaluated the performance of contaminant mitigation of Chinese standard municipal solid waste landfill liner systems. The study was a parametric study comparing the performance of Compacted Clay Liner (CCL) 2m thick (CN1) with that of a composite of Geomembrane (GM) on top of a 1m thick CCL liner (CN2), Fig 3-2. The comparison was done in terms of three parameters: (1) maximum landfill leachate head (y_{\max}) over the liners, (2) leachate rate through liner systems (3) peak concentration and mass of the targeted contaminant (dichloromethane, DCM) discharged in to an aquifer below the assumed landfill. They compared the minimum requirements of Chinese Standard to those of EU and USA. They concluded that the performance of CN1 is less effective in mitigating landfill contamination than CN2 and observed that the minimum design requirement of clay liners in China appears less strict than those of EU and USA.

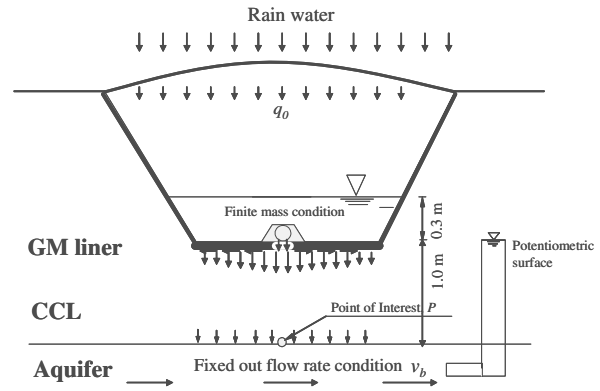


Fig. 3-2 Assumed landfill in which CN 2 liner is used (Du et al 2009)

3.2 Pavements

Han, J. Bhandari and Parsons R.L. USA conducted a micromechanical study to investigate the influence of base course gradation on response of granular bases under cyclic loading. Noting that the satisfactory performance of unpaved roads (roads and rail tracks) depends primarily on the shear strength and stiffness of granular particles and that these two mechanical properties depend on shape, size, and gradation of the particles they observe that the use of a single parameter such as the CBR to characterize the material is inadequate. The study was a simulation study (not a physical test). They described the Discrete Element Method (DEM) modeling using the Particle Flow Code (PFC^{2D}) commercial software using two-dimensional biaxial simulations of uniform sized particles and well graded particles. The results showed that at an identical porosity ($n = 0.16$) and weighted average particle size, the assembly of well-graded particles had a slightly higher angle of internal friction than the assembly of uniform particles. An unreinforced base of well-graded particles performed better than that of uniform particles under cyclic loading. The geogrid reduced the deformation of the granular base. For the geogrid modeled in this study, the reinforced base of uniform particles outperformed the reinforced base of well-graded particles due to the better interlocking between the larger size of particles in the uniform particles.

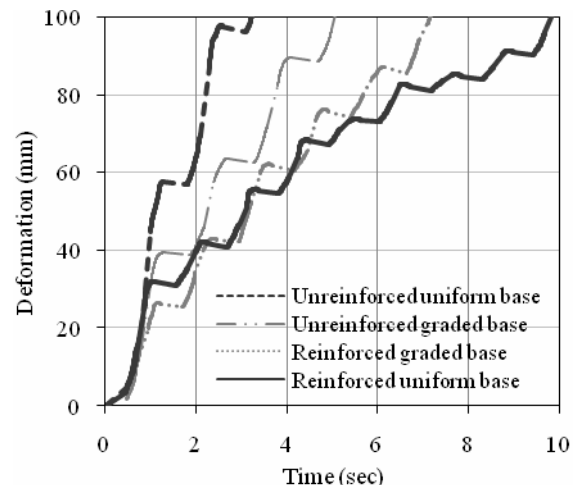


Fig. 3-3 Effect of reinforcement on deformation (Han et al 2009)

Zornberg J.G. & Gupta R. reported on Reinforcement of pavements over expansive clay subgrades. Geosynthetics may be used for basal reinforcement for different reasons. The study reported describes an application of basal reinforcement of pavements for the purpose of mitigating the development of longitudinal cracks induced in pavements constructed over highly plastic, expansive clay subgrades. The study reports on

lessons learned from the performance evaluation of recent projects involving pavement reinforcement projects over expansive clays. They conducted a study of road projects over expansive subgrades in Texas and noted that most of them had problems with pavement cracking and that to address these problems a large percentage of them have resorted to using geosynthetics. They visited several of the projects for post-construction evaluation. They concluded from this evaluation that geosynthetic reinforcements can be used to effectively minimize the development of longitudinal cracks and also to relocate possible longitudinal cracks beyond the reinforced zone. However, they observe that current specification and practice is inadequate to address the various concerns and that the mechanism of action of geosynthetic needs to be investigated further.



Fig. 3-4 Typical longitudinal crack developed on pavements over expansive clays (Zornberg et al 2009).

3.3 Dams

Pimentel V.E. Benjamin C.V.S. Franco D. and Franca P., describe the use of geosynthetics in the elevation of a mining dam in Brazil. The paper is a description of the different application of geosynthetics in one project in order to overcome the constraints on technology use, speed of construction and accurate forecast of volumes of material required. The paper describes the different functions of the Geosynthetics: erosion control, soil reinforcement, drainage and filtration. The Geocells which are thermofixed nonwoven PP strips were used for the bottom and side revetment of the spillway and had concrete infill. The Geogrids were High tenacity polyester geogrids coated with PVC used for enhancement of geotechnical properties of local soil in the main dam. The Geotextile made of non-woven Polyester was used to promote separation between embankment surface and geocells concrete infill.

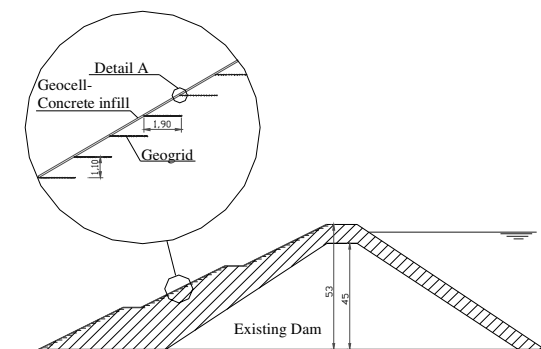


Fig. 3-5 Cross section of the Dam showing different application of geotextiles (Pimental et al 2009)

Beirigo E.A., Gardoni M. G. and Palmeira E.M reported on investigations they had conducted on geotextile specimens exhumed from the drying bay of the Germano tailings dam in Brazil. The tailings disposal technique used in this plant is the process of desiccation. The section showing where the geotextile was placed is shown in Fig. 3-6.

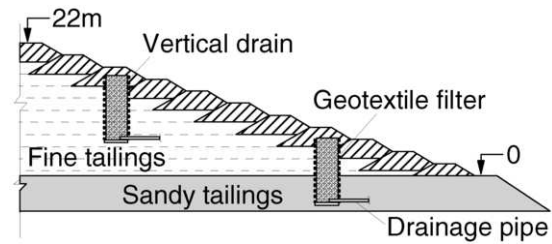


Fig. 3-6 Section of Germano Dam showing Drying bays (Beirigo et al 2009)

The geotextile was a non-woven needle punched and was exhumed from the tailings dam filter system. In addition to the filter samples, tailings material were also taken and tested. The investigations consisted of Physical integrity tests, X-ray diffractometer test, laser beam grain size analyzer and Electron microscopy tests for interaction mechanism between geotextile and adjacent material. They used the ratio between the mass of the particles entrapped in the geotextile and the mass of geotextile fibres per unit area to describe the level of impregnation (λ) of the geotextile by tailings particles. In order to obtain the specimens to be used for the evaluation of the spatial variability of the geotextile mass per unit area and level of impregnation by tailings particles a simple random statistical procedure was adopted. Their results showed that there were different levels of geotextile impregnation by tailings particles but these did not occur in a uniform manner. The microscopic analysis showed local blinding and internal clogging. Consequently there is no clear correlation between the specimen mass per unit area and its impregnation level. Their study highlighted the need for further studies to clarify the effect of the various factors such as local blinding, internal clogging on the filter behavior.

3.4 Embankments on Soft Foundation Soil

Ye Y.S., Cai D.G Zhang Q.L and Yan H.Y., from China presented a paper titled "Calculating method of reinforced bedding in the geosynthetics reinforced and pile supported embankment". They noted that the analysis of this category of structure is complicated by the subgrade "soil arching effect" and "cable/membrane effect". Their study was fundamentally an analytical procedure, however to provide input for their analysis, they conducted a field test in which a 25m thick soft soil has been reinforced with 0.5m diameter concrete piles at 2.5m centres, on top of which is a layer of crushed rock 0.6m thick incorporating a two-dimensional 80kN/m intensity geosynthetics. Though details of the measurement are not given, they compared the stresses between the piles obtained by actual measurement with those predicted by different design procedures and noted that the German procedure appeared to predict the stresses better. They also conducted a model test using a steel pile with polystyrene board as soil and varied the size of the pile cap and geosynthetic strength. Based on the observations as well as results of numerical analysis, they presented an analytical procedure for the computation of the various stresses in the reinforced members. They made a number of recommendations for the design. They observed that the deformation shape of geosynthetics is close to that of a cable and that it should be assumed that vertical load of embankment is borne mainly by the geosynthetics between pile cap. They concluded that the vertical stress caused by arch effect adopts a

spherical arch theory, while the tensile force should be computed by cable theory.

Araujo GLS, Palmeira EM, Cunha RP. One possible solution to the problem of construction on collapsible porous clay is the use of granular columns under the embankment to increase its bearing capacity and reduces vertical displacements. In this paper the authors investigate the use of geosynthetic encased columns in a tropical collapsible porous clay in Brazil. The investigation consisted of a field loading test using polyester woven geotextile filled with sand in a Experimental Foundations Research Site. The piles were 0.4m diameter and 8m long sand piles encased in a seamless woven polyester geotextile bearing in a stiff layer. The sand piles were prepared by pluviation in air. The instrumentation to monitor the load and deformation consisted of a load cell at the top, 3 LVDT for top displacement, six strain gauges at 1.0, 2.5, 4.5 and 6.5m depth and horizontal strain gauges at 1.0 and 4.5m. The strain gauges consisted of electric strain gauges anchored to epoxy disks at its ends. The authors describe an interesting method of maintaining the relative positions of the strain gauges and of ensuring that the installation does not damage the instrumentation. A data acquisition system was used to collect the data. The pile was then loaded and the load settlement curve for the uncased and encased sand columns were plotted. Typical results are shown in Fig. 3-7. The method developed by Decourt (1996) was employed to obtain the bearing capacity of the column defined as the load for which the stiffness is equal to zero on plot of pile load versus loading/settlement index (stiffness).

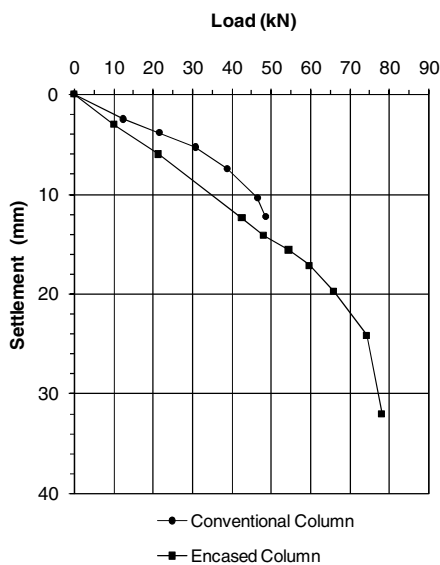


Fig. 3-7 Load-Settlement curves for conventional and encased sand columns (Araujo et al 2009)

Their results showed that the presence of geotextile casing significantly increases bearing capacity from 53kN to 96 kN, an increase of as much as 81%. The strain measurements show that there was greater load transference from the top of the column to its tip in the test with the encased column.

Al-Adili A., Chandra S. Sivakugan N. presented a study on "Slippage effect on the settlement response of a (granular bed -) soft soil system". The problem they modeled is shown in Fig. 3-8. They noted that the presence of the geosynthetics is to increase the load bearing capacity of the soft soils and to improve the settlement performance. They observed that the common methods of analysis use lumped parameter modeling and where numerical methods have been used they considered only single layers of reinforcement or did not consider slippage of reinforcement. The authors therefore presented a numerical

approach to analyze a multi layer geosynthetic-reinforcement that allowed slippage of the geosynthesis.

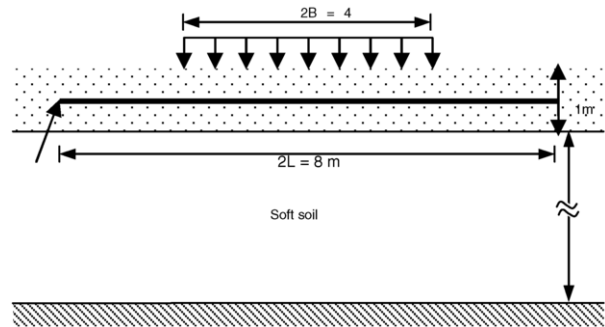


Fig. 3-8 Multi layer geosynthetic-reinforced granular fill over soil

They used the FEM software PLAXIS to predict the settlement. Their results showed among other things that the effect of reinforcement is to reduce the maximum settlement at the centre of the fill by about 11% for a single layer of reinforcement without slippage. The slippage of the reinforcement at the interface of reinforcement and granular soil shows about 5 percent increase in settlement over the case of no slippage.

3.5 Bearing Capacity of Shallow Foundations

Casagrande M. D.T., Consoli N.C. and Thome A. from Brazil investigated the behaviour of plate tests bearing on fiber-reinforced sand. They used Polypropylene fiber of average dimensions; 24 mm in length and 0.023 mm in diameter, with a specific density of 0.91 to reinforce fine sand. The sand was vibratory compacted in a 2.8m x 2.8m x 1.4m high box to a relative density of 90%. The loading plate was 0.3m diameter and the loading was applied by a hydraulic jack monitoring the displacement with LVDT. They observed that fiber reinforcement of sand caused a drastic change to plate load settlement characteristics leading to an increase in the strength and stiffness. In addition they concluded that fiber reinforcement leads to a change in failure mechanism as non-reinforced sand showed "punching" shear failure whereas the mechanism for the fiber-reinforced sand suggests that lateral expansion of the sand is contained by the fibres acting in tension thereby increasing the confining stresses and leading to higher load bearing capacity.

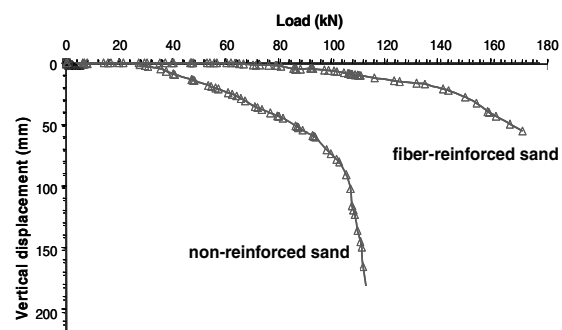


Fig. 3-9 Load-settlement behaviour observed for non reinforced sand and fiber-reinforced sand (Casagrande et al 2009).

Zhusupbekov A, Lukpanov R., Muzdybaeva T. Das B.M. Patra C.R. Shin E.C., from Kazakhstan conducted a study titled "Bearing capacity of eccentrically loaded strip foundation on geogrid-reinforced sand" They conducted a physical model test on an 80mmx360mm strip footing made of Steel plate whose base has been roughed by coating with glue and sand. The model box was 0.8m x 0.365m x 0.7m, polished in the inner

surface to reduce friction and braced to avoid lateral yielding. The sand was compacted to a relative density of 71% corresponding to $\gamma_{bulk}=14.81N/m^3$, and $\phi=41^\circ$. The geogrid was placed in the sand in multiple layers.

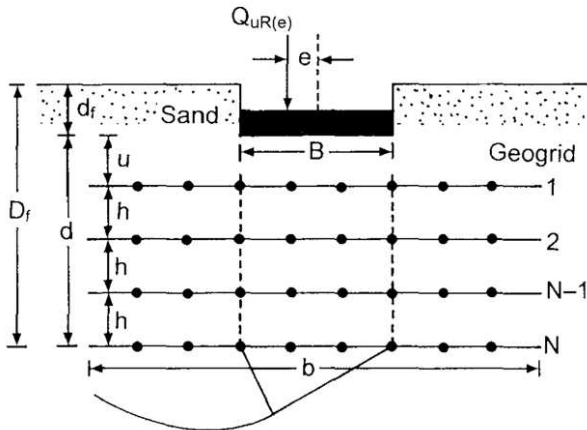


Fig. 3-10 Assumed failure mode under an eccentrically loaded strip foundation on geogrid-reinforced sand (Zhusupbekov et al. 2009)

The study focused on evaluating the effect of eccentric loading with eccentricity varying from 0 to 0.15 and effect of depth of embedment from surface loading to $d_f/B=1$. The study assumed that bearing capacity of an eccentrically loaded column $q_{uR(e)}$ and that of a centrally loaded footing q_{uR} are related through a reduction factor R_{KR} which is a geometric function of the eccentricity and the depth factor of reinforced ground as given equations 3-1 and 3-2

$$\frac{q_{uR(e)}}{q_{uR}} = 1 - R_{KR} \tag{Equation 3-1}$$

$$R_{KR} = \beta_1 \left(\frac{D_f}{B} \right)^{\beta_2} \left(\frac{e}{B} \right)^{\beta_3} \tag{Equation 3-2}$$

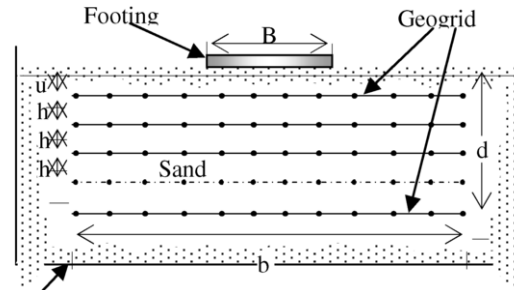
By running a total of 20 tests with varying values of e/B for fixed D_f/B and vice versa, and plotting the results they obtained the values of the coefficients as $\beta_1=5.11$, $\beta_2=-0.14$ and $\beta_3=1.21$ and thus mathematically evaluated the effect of eccentricity and depth of reinforced ground on the bearing capacity.

Nakai T. Shahin H.M., Watanabe A and Yonaha S. from Japan investigated the "Reinforcing mechanism of geosynthetics on bearing capacity problems-model tests and numerical simulations". The study sought to throw more light on the reinforcement mechanism so as to help establish a rational design method of reinforced-soil ground. They used a two-dimensional laboratory model test and numerical analyses. For the physical model test the footing was 12cm wide and there was provision for measuring the vertical and rotation of footing with dial gauges. They used a synthetic ground made of Aluminium rods (1.6mm, 3.0mm dia.) to represent sand while the reinforcing material was tracing paper. Both rough and smooth reinforcement were investigated. The variables used in the test were installation depth, D, Length of reinforcement, L, skin friction, δ of reinforcement. The distribution of shear strain of the model tests are obtained from the simulation of Particle Image Velocimetry (PIV) technique taking two photographs before and after loading.

For the analysis they used an elastoplastic subloading t_{ij} model (Nakai & Hinokio, 2004). The study concluded that the effectiveness of reinforcement depends on the position of reinforcement and its skin friction. Specifically, no extra reinforcement effect is seen when placed deeper than $D/B=1/2$

and when the reinforcement is placed on the ground surface just below the foundation, there is almost no effect of the reinforcements. The numerical analysis confirmed the results of model test.

Puri V.K. Kumar S. Das B.M. Prakash S. and Yeo B. in USA investigated the settlement of reinforced subgrades under dynamic loading using model tests. The model footing was a square footing of side 76.2cm with a rough base (made by cementing sand grains) loaded in a plexiglas cubic box of side 760cm, reinforced on the sides to prevent yielding.



Test Tank

Fig. 3-11 Test set up (Puri et al. 2009)

A layer of foam was glued to the bottom of the box to prevent effect of reflected waves on settlement. The sand was prepared to a relative density of 70% by pluviation and reinforced with biaxial PP/HDPE co-polymer geogrid.

The test programme consisted of 2 phases. In the first phase they determined critical values for b/B and d/B by varying the number of reinforcement N from 1 to 6 for $b/B=6$ and then varying the value of b/B for $N=4$. From these tests they concluded that $b/B=(b/B)_{cr}=4$; and $d/B \approx (d/B)_{cr}=1.33$. In the second phase they applied the dynamic load q_d of magnitude $q_d/q_u=4.36-22.33\%$ at 1 Hz under a static pressure, q_s of magnitude $q_s/q_u=13.2-33.3\%$ and monitored the load settlement curve. The plot of the normalized settlement against the load cycles is shown in Fig. 3-12. They observed that for each dynamic load there is a critical number of load cycles beyond which increase in settlement was small

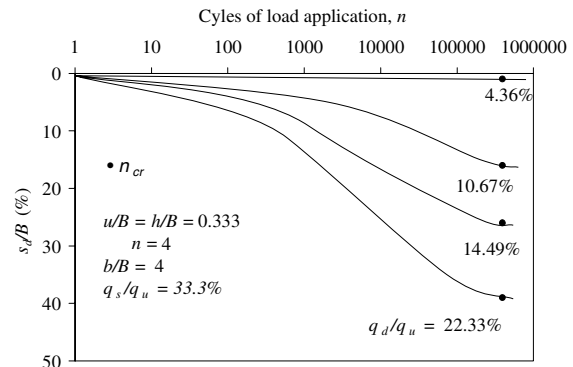


Fig. 3-12 Variation of s_d/B with n (Series II-C)

They concluded that maximum mobilization of bearing capacity for a given sand-geogrid system occurs with optimum values of $b/B=(b/B)_{cr}=4$; and $d/B \approx (d/B)_{cr}=1.33$. For a given sustained stress and number of load cycles, the settlement due to dynamic loading increases with increase in magnitude of dynamic stress. For given values of dynamic stress and number of load cycles, the dynamic settlement increases with increase in magnitude sustained static stress.

3.6 Reinforced Soil Wall

Sayao ASFJ Nunes ALLS, Becker LDB and Siera ACCF from Brazil investigated the behaviour of geogrids under pull out

tests in fine and coarse soils. They noted that most design criteria neglect cohesion and therefore clean sandy soils are commonly used. The authors investigated the behavior of geogrids interfacing with fine weathered residual soils.

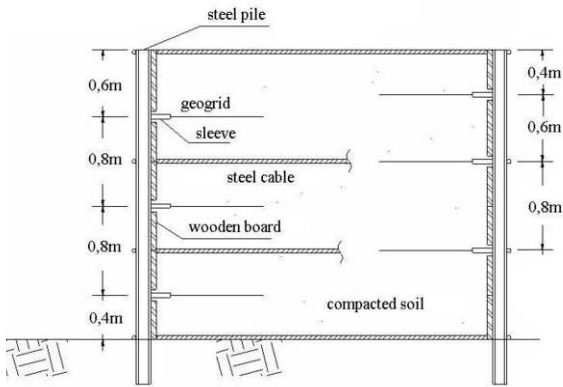


Fig. 3-13 Experimental fill for pullout tests of geogrids (Sayao et al 2009)

They used both field and a laboratory pull out tests. For the field pull out test they constructed 2.6m x3.5m x10.8m fill supported by vertical steel members and filled it with compacted clayey silt of residual origin ($\phi=34-43$, $c=6-12\text{kPa}$) In one half of the fill the soil was compacted to 95-100% Standard Proctor at +/-2% OMC and reinforced with 18 geogrid specimens. In the other half it was compacted to +2% to +4% OMC at 95% Standard Proctor and reinforced with 6 geogrid specimens. Displacement transducers were positioned along the grid specimen. The laboratory pull-out test was conducted in a rigid shear box 1m x1m x1.2m filled with compacted silty clay at compaction degree of 95% and water content of $16 \pm 0.2\%$. ($\phi=21$, $c=30\text{kPa}$) and reinforced with woven geogrid. At the maximum pull out load, the mobilized length, L_{mob} , was defined as the geogrid's section with displacements larger than 1mm. The equivalent average mobilized shear strength, τ_{mob} is related to the maximum pullout load per unit width, T_{max} through Equation 3-3.

$$\tau_{mob} = \frac{T_{max}}{2.L_{mob}} \quad \text{Equation 3-3}$$

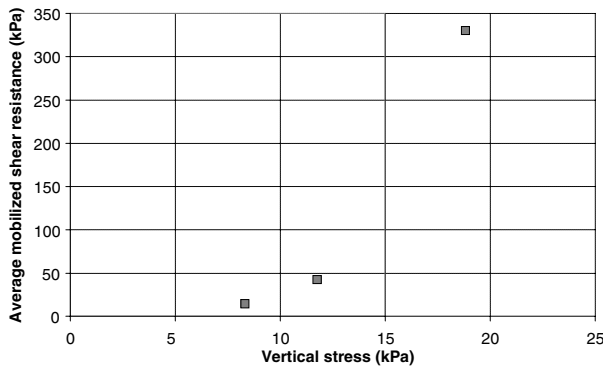


Fig. 3-14 Mobilized shear resistance vs. vertical stress for field test (Sayao et al. 2009)

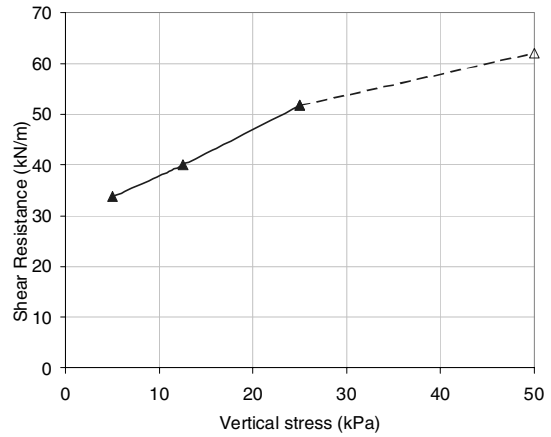


Fig. 3-15 Strength envelope from laboratory pullout tests (Sayao et al. 2009)

They observed that both field and laboratory results showed tensional strains decreasing along the grid specimen indicating non-uniformity of the soil's mobilized shear strength. However, the strength envelope obtained in the field (Fig. 3-14) and that obtained in the laboratory (Fig. 3-15) are different.

Luking J. and Kempfert H.G. from Germany reported on their study title "Load bearing behaviour of geotextile containers using Velcro strips Geotextile containers". They noted that geotextiles containers are produced predominantly of non woven geotextile and they come in different forms and dimensions. They have a wide range of applications from scour and erosion protection at beaches to groynes and breakwater walls and supporting structure for slopes. The stability of a geotextile container construction depends on several factors especially the friction between the containers. The authors therefore performed model tests and numerical analysis to investigate the effect of velcro strips between each container layers. The used element shear box test, model test and numerical analysis using FEM programme PLAXIS-8.2. For the shear box element test the velcro strips were sewn to the geotextile and installed in the middle of the test specimen. They investigated different Velcro strips, different geotextiles, different interface moisture conditions. In addition to the element test they conducted an experimental Model Test using 26 containers each filled to 80% of its capacity with and without Velcro strips. The layout is shown in Fig. 3-16.

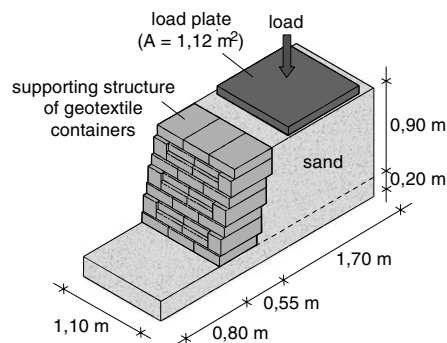


Fig. 3-16 Schematic view of the model test (Luking & Kempfert, 2009)

They observed increase in load bearing capacity using Velcro strips but the increase depends on type of Velcro strips used. They also observed that pollution of surface reduces effectiveness of Velcro strips. The deformation predicted by FEM was about 4 times smaller than that measured in the model. This was flagged as an area that require further investigation.

Hatf N. and Sadr A. from Iran presented the study titled “Pull-out behaviour of an innovative grid anchor system” which was an evaluation of performance of a new type of anchor which they refer to a “Grid-Anchor”. They investigated the performance using laboratory element test and finite element analysis. For the laboratory test they constructed a Steel box 35cm x30cm x35cm and used a well graded sand ($\phi=43^\circ$) and provided a system for application and measurement of vertical and horizontal loads. For the pull-out test they measured the clamp displacement as well as relative force at 5 overburden pressures, 4,8,12 and 18kPa for each reinforcement. Part of their results comparing the performance of the new “grid-anchor” to that of normal geogrid using the results of the laboratory test is shown in Fig 3-17.

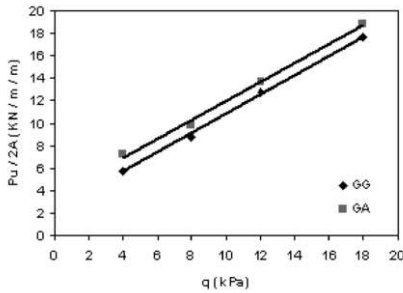


Fig. 3-17 Relationship between ultimate pull-out stress ($P_u/2A$) and overburden pressure (Hatf and Sadr, 2009)

The results showed the same friction angle for new “grid-anchor” and normal geogrid which implies that the anchors did not have any influence on friction component of geogrid, but the magnitude of the friction angle of both reinforcements of 60° is 40% higher than the internal friction angle of unreinforced soil of 43° . They also performed pullout simulation using FE code (PLAXIS-2D) and their Numerical analysis showed that the whole length of reinforcement does not experience elongation and recommended that arrangement of anchor group be as close to the active end as possible.

3.7 General Application

Khan A.J., Siddiquee MSA, Noor MA. Mahaseth B., working from Bangladesh reported on the Isothermal response of geosynthetics to a multi stage loading. They observed that even though the geosynthetic reinforced soil walls and slopes were not designed for the high earthquake forces they experienced most of them performed satisfactorily during the 1994 Northridge, California earthquake and 1995 Kobe earthquake. For the design of GRSSs for earthquake loadings, the reference strengths obtained from constant rate of strain test (CRS) are enhanced by a modification factor of 1.5 of doubtful technical basis. The authors sought to investigate the load-strain behaviour of geosynthetic under such multi-stage loading (MSL), i.e. under combined sustained plus short-term earthquake loading in the current design methods. They presented an analytical Method for geosynthetics under both single stage loading (SSL) and Multistage loading i.e. combination of sustained and earthquake loading. They postulated that Geosynthetics when loaded, the ratio of recoverable elastic strain, ϵ_R , and locked-in strain (ϵ_L =the plastic strain + viscous strain) to reach a particular limiting strain is unique. They then went on to propose a design approach that incorporates the concept of “available strain” defined as the difference between the limiting strain (failure criteria) and strain just before an event.

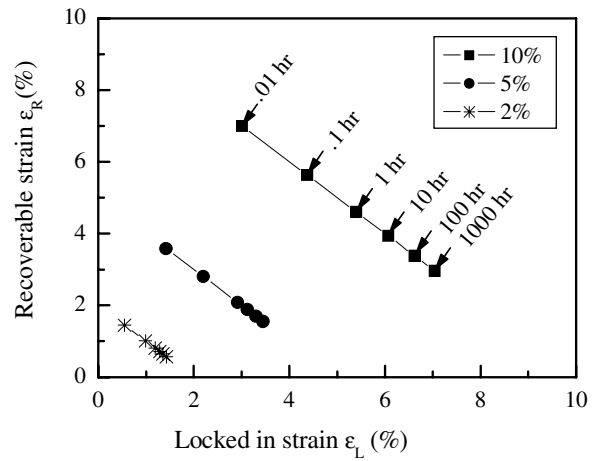


Fig. 3-18 Strain envelop at different strain levels for the geogrid at 20°C (Khan et al 2009)

Atmtzidis D.K., Chrysikos DA and Papaefstathion IM from Greece investigated installation damage of nonwoven polypropylene geotextiles. Installation damage is one of the three factors for which reduction factors are applied to laboratory determined strength of geotextiles for design purposes. They observed that difficulties arise with field tests due to the numerous factors that affect the results and existing laboratory generated results are limited due to the small number of geosynthetics tested per reported investigation and provides no correlations between installation damage and geosynthetic physical and/or mechanical properties. Their study therefore sought to provide a quantitative evaluation of installation damage of nonwoven polypropylene geotextiles based on results obtained for a relatively large number of samples tested according to standard procedures. They used a custom constructed loading equipment and conducted two series of tests; the first series used standard ENV ISO 10722-1 procedures with synthetic aggregates made from commercially produced Aluminium oxide with angular grains. The second series was a modified testing procedure with Electric arc furnace slag and Crushed limestone as aggregates and loading cycles ranging from 100 to 400. All geotextiles were nonwoven, polypropylene, needle-punched and were made of staple fibers. The installation Damage was determined with wide width tensile test and visual inspection of geotextile after test. They computed the percent retained tensile strength and failure deformation and correlated them with the Mass per unit area of the geotextile. Parts of their results are summarized in Fig 3-19. Their results showed that the effect of installation damage is not significant for geotextiles with mass per unit area over 500g/m^2 . Los Angeles coefficient of aggregate is not a good indicator of damage potential to geotextile.

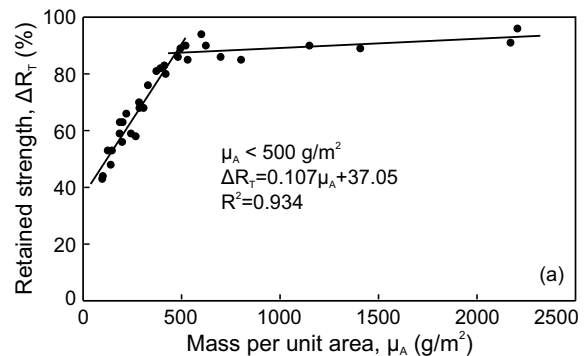


Fig. 3-19 Correlation between geotextile mass per unit area and retained tensile strength, (Atmtzidis, et al. 2009)

They concluded that with installation damage reduction factor values of 1.05-1.20 for geotextiles with mass per unit area greater than 500g/m², and 1.20-2.10 for geotextiles with lower mass per unit area, the results of their study are in very good agreement with the recommended values

El-Sherbiny R. and Gross B., investigated the design service life of geogrids in mechanically stabilized earth walls. The authors presented the factors affecting durability and service life of geogrid reinforcement used in MSE walls as applied in landfill systems. The current design approach used to account for strength losses due to construction damage, creep, and long-term degradation is to apply reduction factors to the ultimate tensile strength (T_{ult}) of the reinforcement. The allowable strength (T_{al}) is then calculated using the equation 2-1:

$$T_{al} = \frac{T_{ult}}{RF_{CR} \times RF_{ID} \times RF_D} = \frac{T_{ult}}{RF} \quad \text{Equation 3-4}$$

where: RF_{CR} = creep reduction factor; RF_{ID} = installation damage reduction factor; RF_D = degradation reduction factor; and RF = product of all applicable reduction factors.

They noted that the Reduction factors commonly used in design were developed for road embankment applications and generally reflect a 100-year service life. The paper presents a method to account for the design service life of the geogrid reinforcement. The approach is to use the results of accelerated creep tests conducted at elevated temperatures to infer creep for an additional order of magnitude using time-temperature superposition principles. They used data from creep tests on the HDPE geogrid, at temperatures ranging from 20°C to 40°C (Anderson, 2006) and superimposed data from creep tests on the PET geogrid at temperatures ranging from 20°C to 60°C. Both data are time shifted to a reference temperature of 20°C. From the figure they back-calculated creep reduction factors for service lives of 100, 200, and 500 years. Their conclusions are shown in Table 3-1.

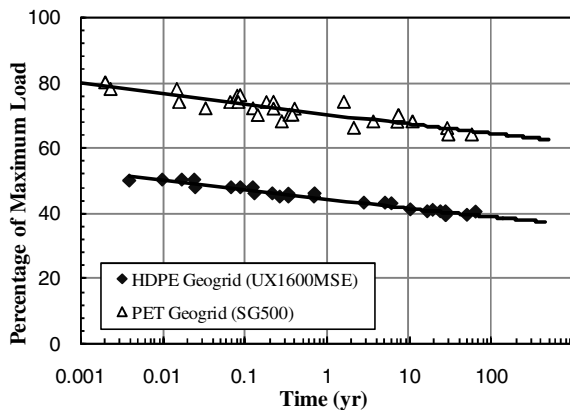


Fig. 3-20 Stress-Rupture Test Results at a Reference Temperature of 20°C for an HDPE and a PET geogrid (El-Sherbiny et al 2009)

Table 3-1. Strength Reduction Factors for Geogrid.

Geogrid	Design Service life (years)	Installation Damage Red. Factor RD _{ID}	Creep Red. Factor RD _{CR}	Degradation Red. Factor RD _D	Overall Red. Factor RF
HDPE Uniaxial Geogrid	100	1.1-1.45 ¹	2.65-5.0 ¹	1.1 ¹	3.2-8.0
	100	1.12 ²	2.57 ²	1.1 ²	3.2
	200	1.12 ²	2.62 ²	1.1 ²	3.2
	500	1.12 ²	2.69 ²	1.5 ²	4.5
PVC Coated PET Geogrid	100	1.1-1.85 ¹	1.6-2.5 ¹	1.15-1.3 ¹	2.0-6.0
	100	1.29 ³	1.61 ³	1.1 ³	2.3
	200	1.29 ³	1.64 ³	1.15 ⁴	2.4
Acrylic Coated PET Geogrid	100	1.29 ³	1.68 ³	1.3 ⁴	2.8
	100	1.2-2.05 ¹	1.6-2.5 ¹	1.15-1.3 ¹	2.2-6.7 ¹

Notes: ¹ Elias et al. (2001), ² For UX1600MSE, ³ For SG500. ⁴ Durability reduction factor for PET (Risseeuw and Schmidt, 1990).

Carneiro J.R., Almeda, P.J. and Lopes M.L. investigated “Natural weathering of geosynthetics in Portugal”. They noted that geosynthetics by reason of their application are exposed to several degradation agents, such as: ultraviolet (UV) radiation and other weathering agents, high temperatures, atmospheric oxygen, acids, alkalis or microorganisms. Being polymeric products UV can induce the formation of highly reactive free-radicals which in the presence of oxygen, can attack the polymeric chains of the GSs. This degradation process is usually accelerated by high temperatures and by the existence of high moisture contents on the materials. They noted that laboratory weatherometer tests are limited by the test duration and also by the fact that they cannot take the effect of factors such as wind, dirt or chemical pollutants into account. They used three groups of geosynthetics: needle punched non-woven polypropylene geotextiles GTX, woven HDPE Geonet (GNT) and HDPE) Geomembrane (GMB). These were exposed to weather for periods up to 24 months. They used Tensile Testing on 200mmx50mm specimens for GTX and GNT and dumbbell shaped specimens of GMB and Scanning Electron Microscopy (SEM) for all specimens. GTX and GNT damage were evaluated using tensile strength (TS) and elongation at maximum load E_{ML}, but GMB degradation was evaluated by tensile strength at yield TS_{YIELD}, tensile strength at break (TS_{BREAK}), elongation at yield E_{YIELD} and Modulus of Elasticity (ME). Their results showed that the PP GTX was seriously affected by exposure to weather losing complete strength in 24 months. SEM analysis showed fibre perpendicular to GTX plane broken and transversal fissures on in-plane fibre. They observed that addition of chemical additives such as carbon black improved its resistance to UV. HDPE GNT and GMB presented good resistance to weathering

Mendez B. Botero E. and Romo M.P. from Mexico reported their investigation that sought to extend the applications of fibre reinforced polymers into design of the pad of a shaking table for geotechnical application. The pad was made of Kevlar fibre-reinforced polymers. The KFRP was a composite material formed with a plywood core reinforced with Kevlar fabric in an epoxy resin matrix. They conducted static and dynamic bending tests on the new material. They concluded that the new composite material has several advantages over traditional material such as steel and aluminium.

Kavazanjian E. Jr Iglesias E and Karatas I from USA reported on “Biopolymer soil stabilization for wind erosion”. The authors noted that fine-grained airborne soil particles especially particles with a nominal size of 10 micrometers or less (PM-10), can penetrate deep into bronchial tubes and can cause serious health problems. Consequently, the United States (US) Environmental Protection Agency (EPA) uses airborne PM-10 concentration as an air quality indicator and areas that exceed the US National Ambient Air Quality Standard for PM-10 are designated as “non-attainment” zones. Construction activities are one source of increased airborne PM-10 concentrations and conventional dust control techniques at construction sites include frequent watering of the soil and application of cover materials and chemical stabilizers. The authors present a study into the use of a bio-polymer that has the potential to be used as stabilization against wind-induced erosion. The authors prepared samples of non-plastic silty sand and stabilized it with two bio-polymer stabilizers: chitosan and xantan gum. In the first test they mixed the bio-polymer and compacted. In the second test they sprayed the biopolymer emulsion on the surface of soil. Then they conducted wind tunnel testing to measure the weight loss on exposure to 26km/hr wind. They also tested control samples prepared using untreated soil and soil treated with water without any biopolymer additive. Their investigation showed that both biopolymers were effective stabilizing agents against wind

erosion and both spray-on and mixing before compaction were effective. They also found that the biopolymers were effective when exposed to UV radiation and summer temperatures but they broke down for spray-on against 105°C temperature. They recommended that additional testing be carried out to establish the cost-effectiveness of biopolymer stabilization and to establish the durability when exposed to surface water flow and infiltration and when subject to wetting and drying cycles.

REFERENCES

Papers in this Session

- Adamska K.Z and sulewska M.J., 2009, Neural modeling of CBR values for compacted fly ash
- Ajdari M. Habibagahi G. and Ghahramani A., 2009, Predicting effective stress parameter of unsaturated soils in plane strain condition using neural networks
- Al-Adili A., Chandra S. Sivakugan N., 2009, Slippage effect on the settlement response of a (granular bed -) soft soil system
- Al-Farouk O. Al-Damiuji, Al-Omari R.R. Al-Ani, M.M. Fattah M.Y., 2009, Experimental and numerical investigation of dissolution of gypsum in gypsisferrous Iraqi soils
- Al-Khafaji AN, Khorshid NS, Al-Musawe MJ, Al-Obaid BM, 2009, Deformability of gypseous soil in Iraq
- Araujo GLS, Palmeira EM, Cunha RP., 2009, Geosynthetic encased columns in a tropical collapsible porous clay
- Arthurs JM, Wilson CJN and Prebble WM, St. George, JD., 2009, Sensitivity in volcanoclastic silts in North Island, New Zealand
- Atmtzidis D.K., Chryssikos DA and Papaefstathion I.M., 2009, Installation damage of nonwoven polypropylene geotextiles
- Badillo E.J., 2009, Mathematical characterization of pumice and quartz sands
- Beirigo E.A., Gardoni M. G. and Palmeira E.M., 2009, Investigations on geotextile specimens exhumed from a mining tailings dam
- Bicalho K.V. Marinho FAM Fleureau J.M. Correia A.G. and Ferreira S., 2009, Evaluation of filter paper calibrations for indirect determination of soil suctions of an unsaturated compacted silty sand
- Carneiro J.R., Almeda, P.J. and Lopes M.L., 2009, Natural weathering of geosynthetics in Portugal
- Casagrande M. D.T., Consoli N.C. and Thome A. 2009, Behaviour of plate tests bearing on fibre-reinforced sand
- Demeneghi A., 2009, Deformations assessment in expansive clays
- Du, Y.J., Liu, S.Y. and Shen S.L. 2009, Evaluation of the performance of contaminant mitigation of Chinese standard municipal solid waste landfill liner systems
- El-Sherbiny R. and Gross B., 2009, Design service life of geogrids in mechanically stabilized earth walls
- Farooq J and Virk K.A., 2009, Improvement of engineering characteristics of expansive clays in sand mixing
- Frangov, G., Krastonov. M. and Varbanov. B., 2009, Complex engineering geological conditions for civil construction in the Rhodope Mountain (Bulgaria)
- Han, J. Bhhandari and Parsons R.L., 2009, Influence of base course gradation on response of granular bases under cyclic loading: a micromechanical study
- Hassanlourad M. Salchzadeh H. and Shahnazari H., 2009, Strength of chemically grouted micro pile model in calcareous sand
- Hatf N. and Sadr A., 2009, Pull-out behaviour of an innovative grid anchor system
- Imre, E. Moczar, B and Farkas J. 2009, Laboratory creep and relaxation after partial unloading
- Ishikawa T., Miura S. and Tokoro T., 2009, Effect evaluation of freeze-thaw action on hydromechanical behaviour of unsaturated granular materials
- Kavazanjian E. Jr Iglesias E and Karatas I., 2009, Biopolymer soil stabilization for wind erosion control
- Khan A.J., Siddiquee MSA, Noor MA. Mahaseth B., 2009, Isothermal response of geosynthetics to a multi stage loading
- Kikkawa N. Pender M.J., Orense R.P. and Matsushita E., 2009, Behaviour of pumice sand during hydrostatic and Ko compression
- Li, L. Wang S.J. Chen R., Ng C.W.W. and Li Z., 2009, The reinforcement mechanism and effect of potassium silicate solutions in an unsaturated loess soil subjected to saturation.
- Luking J. and Kempfert H.G., 2009, Load bearing behaviour of geotextile containers using Velcro strips
- Mazzieri F., Pasqualini E. DiEmidio G., Van Impe W.F., 2009, Hydraulic conductivity of a dense prehydrated GCL subjected to partial desiccation
- Medeiros C. Jr, Drosemeier A. C.C. Muxfeldt A.S., Dutra A.B. Silveira C.A.B. and Sants R.M., 2009, Geotechnical characterization of calcareous soils for the foundation design of offshore production platforms
- Meier C. Boley C. and Zou, Y., 2009, Practical relevance of collapse behaviour and microstructure of loess soils in Afghanistan
- Mendez B. Botero E. and Romo M.P. 2009, A shaking table pad made of Kevlar fibre-reinforced polymers
- Nakai T. shahin H.M. Watanabe A and Yonaha S. Reinforcing mechanism of geosynthetics on bearing capacity problems-model tests and numerical simulations
- Nowamooz h. and Masrouri F., 2009 Hydromechanical behaviour of expansive soils during the wetting and drying cycles (in French)
- Okajima K. Tanaka T Zhusupbekov A, Baitassov T. Bazarbayev D. and Popov V., Elasto-plastic FEM model for researching of problematic soil ground of St. Petersburg city
- Omotosho O. 2009, Active soils of the Niger Delta
- Pimental V.E. Benjamin C.V.S. Franco D. and Franca P., 2009, Use of geosynthetics for the elevation of a mining dam construction in Brazil
- Pitanga, H.N. Vilar O.M. and Goure J.P. 2009, Compacted soil shear strength characterization on inclined plane test
- Puri V.K. Kumar S. Das B.M. Prakash S. and Yeo B., 2009, Settlement of reinforced subgrades under dynamic loading
- Reiss R.M., Vilar O.M. and Azevedo R.F., 2009, Stress-strain behaviour of a residual soil profile from gneiss
- Rinaldi V.A. and Capdevila J.A. 2009, Effect of sampling disturbance on the stress strain behaviour of a saturated collapsible soil
- Rojas J.C. and Mancuso C., 2009, Effect of loading rate on the behaviour of unsaturated soils
- Sayao ASFJ Nunes ALLS, Becker LDB and Siera ACCF., 2009, Behaviour of geogrids under pull out tests in fine and coarse soils
- Szymanski A., Sas W. and Niesiolowska A., 2009, Field and laboratory experience with the soft subsoil deformation
- Taibi S., Dumont M. and Fleureau J.M., 2009, Effective stress extended to unsaturated soils-effect of the interfaces parameters (In French)
- Villar LFS, de Campos TMP, Azevedo R.F. Zornberg J.G., 2009, Tensile strength changes under drying and its correlations with total and matric suctions
- Ye Y.S, Cai D.G Zhang Q.L and Yan H.Y., 2009, Calculating method of reinforced bedding in the geosynthetics reinforced and pile supported embankment
- Zhakulin AS Zhakulina AA and Unaibaev B.Zh., 2009, Consolidation of the multilayered soil basis
- Zhusupbekov A, Lukpanov R., Muzdybaeva T. Das B.M. Patra C.R. Shin E.C. 2009, Bearing capacity of eccentrically loaded strip foundation on geogrid-reinforced sand
- Zornberg J.G. & Gupta R., 2009, Reinforcement of pavements over expansive clay subgrades

Other References

- Vargas M 1953 Some Engineering Properties of Residual Soils occurring in Southern Brazil Proc. 3rd ICSEF, Zurich Vol1, pp 67-71
- Deere, D.U & Patton F.D., 1971 Slope Stability in Residual Soils, State of the Art Report IV COPAMSEF, Puerto Rico Vol. 1 pp87-120
- Rohm S.A. & Villar O.M., 1995 Shear Strength of an unsaturated sandy soil. Proc. Of the 1st International Conference on unsaturated soil, Paris, Vol. 1, pp 189-193
- Chandler, R. J., Crilly, M. S. and Montgomery-Smith, G. 1992. A low-cost method of assessing clay desiccation for low-rise buildings. Proc. Instn. Civ. Engrs Civ. Engng. 92, May, 82-89
- ASTM Standard D5298-03, 2007, "Standard Test Method for Measurement of Soil Potential (Suction) Using Filter Paper." Annual Book of ASTM Standards, Soil and Rock (I), Vol. 4, No. 8, ASTM International, West Conshohocken, PA
- Fleureau, J.-M., Hadiwardoyo, S., Dufour-Laridan, E. Langlois, V. and Gomes Correia, A., 2002, Influence of suction on the dynamic properties of a silty sand. *Unsaturated Soils*, Jucá, de Campos and Marinho (eds), Sweets and Zeitlinger, Lisse, 2, 463-471